Mechanical properties, nanoscale characteristics, and environmental analysis of high-volume waste coral powder mortar (HVCM)

Zhi-hai He[1,2], Ya-qian Ni[1], Yu Zhang[3], Jin-yan Shi[3,4*], Víctor Revilla-Cuesta[5], Shi-gui Du[6]

[1] College of Civil Engineering, Shaoxing University, Shaoxing 312000, China

[2] Key Laboratory of Rock Mechanics and Geohazards of Zhejiang Province, Shaoxing 312000, China

[3] School of Materials Science and Engineering, Southeast University, Nanjing 211189, China

[4] School of Civil Engineering, Central South University, Changsha 410075, China

[5] Department of Civil Engineering, Escuela Politécnica Superior, University of Burgos, c/ Villadiego s/n, 09001 Burgos, Spain

[6] School of Civil and Environmental Engineering, Ningbo University, Ningbo 315211, China

Abstract: With the development of marine resources, coral-based cement compositions have broad application prospects in coastal infrastructure construction such as island reef construction, flood control embankment, airport, and road, etc. Waste coral powder (CP) was used to prepare high-volume CP mortar (HVCM), and its multiscale characteristics and environmental benefits were assessed, such as strength, microstructure, and nanoscale characteristics. The results showed that with the increase of CP substitution level, the mechanical properties of HVCM decreased, and the autogenous shrinkage of the mixture was significantly improved. The use of CP to replace the high-volume cement degraded the microstructure of the samples. From the perspective of nanoscale characteristics, the incorporation of CP reduced the content of hydration phase in the matrix and increased the pore phase. Meanwhile, the widening of the interfacial transition zone of the HVCM samples was also the main reason for their performance degradation. Although the incorporation of CP decreased the average elastic modulus of C-S-H and increased its total porosity, the pore structure of the gel was slightly refined. In addition, HVCM had lower carbon emissions and consumption of non-renewable energy compared to plain mortar.

Keywords: Mortar; Waste coral powder; Environmental analysis; Multiscale characteristics; Nanomechanical properties

*Corresponding author. jinyan.shi@csu.edu.cn +86-17877780451 (Jinyan Shi).

1. Introduction

With the development of the ocean by human beings, there are more and more marine infrastructure construction projects such as island and reef construction, marine port terminals, and cross-sea bridges [1]. Concrete materials are still the main building materials for marine engineering construction, but there are few raw materials available for concrete production locally [2]. Generally speaking, the binders and aggregates required for marine concrete are transported from the mainland, which greatly increases the cost and energy consumption of raw materials [3,4]. Therefore, it is particularly important to seek alternative raw materials, which are beneficial to reduce concrete costs, fossil energy consumption and CO_2 emissions.

With the implementation of the carbon neutral strategy, it is imperative to reduce the carbon emissions of the construction industry [5,6]. Among the components of concrete, cement has the highest cost and carbon emissions, so it is necessary to seek novel binders suitable for marine concrete [7]. At present, incorporating supplementary cementitious material (SCM) to cement-based materials is an effective approach to decrease cement consumption [8]. Incorporating appropriate amount (~30%) of fly ash, slag and limestone powder to concrete can improve the long-term performance of concrete [9,10]. To further reduce carbon emissions and cost of mixtures, the concept of high-volume SCM-cement composition is proposed [9,10]. For example, high-volume fly ash-based cement components have better fluidity, lower hydration heat release and lower shrinkage deformation, which provides the possibility for the preparation of massive concrete and pumped concrete [9]. Wang et al. [10] also found that high-volume limestone powder has similar properties to high-volume fly ash for concrete in improving volume stability and inhibiting hydration temperature rise. The main composition of limestone powder is calcium carbonate, which also promotes cement hydration and provides nucleation sites for hydration products [10,11]. Meanwhile, limestone powder reacts with tricalcium silicate and calcium aluminate to form calcium carbosilicate hydrate and calcium carboaluminate [7,10]. In addition, incorporating an appropriate amount (20%) of limestone powder is also beneficial to improve the pore structure of the mortar, and reduce the carbonization depth and steel corrosion ratio [12]. Therefore, it is feasible to use calcium carbonate-based SCMs to prepare high-volume SCM cement-based materials. However, there is an urgent need to find a novel SCM suitable for the production of marine cement-based materials.

A large amount of coral waste is generated during construction and development in the open sea (tropical), such as channel dredging, wharf construction and oil well platform construction [13,14]. The chemical composition of waste coral and limestone powder is similar, both of which are calcium carbonate minerals, but the former is mainly aragonite, while the latter is mainly calcite [7,15,16]. Researchers have used coral as aggregate in cement-based materials as early as half a century ago [17]. However, due to the porous character of coral aggregates, it tends to reduce the fluidity, mechanical properties and impermeability of cement-based materials [18]. Therefore, some researchers try to prepare SCM from coral waste and apply it to cement-based materials [7,8]. Shi et al. [7] systematically studied the effect of coral powder (CP) on the properties of cement paste, and concluded that the incorporation of CP was beneficial to the increase of the early-ages (1–7 d) strength of the sample and the refinement of the pore structure, but it had a negative effect on the total porosity and long-term (28–90 d) strength. Meanwhile, CP was able to react with tricalcium aluminate (C_3A) to form hemicarbonate and monocarbonate, which inhibited the conversion of AFt to AFm [7]. Furthermore, Liu et al. used seashells to prepare calcium carbonate-based SCM and found that it exerted higher chemical reactivity in cement-based materials compared to limestone powder [19]. Therefore, CP as a biomass calcium carbonate has the potential as SCM. Meanwhile, the current research mainly focuses on the effect of CP on the mechanical properties of cement-based materials, while the effect of high-volume CP on the multi-scale characteristics of cement-based materials has not been explored.

The purpose of this work is to investigate the technical and environmental feasibility of using high-volume CP to prepare marine cement mortars. Meanwhile, the mechanical properties, shrinkage behavior and multi-scale microstructural characteristics of high-volume CP mortars (HVCM) are investigated. In addition, the carbon emissions and non-renewable energy consumption (NREC) of the mixture are compared to evaluate its environmental benefits.

2. Materials and experiments

2.1. Raw materials

P.O 42.5 cement (OPC) is used in this study, which is provided by Zhaoshan Building Materials Co., Ltd. The waste coral aggregates are collected in the South China Sea, and are respectively crushed, ground and sieved to obtain CP with a particle size of less than 75 μm, as presented in Fig. 1. The chemical compositions of OPC and CP are presented in Table 1, and CaO is the main oxide

component of CP, which provides its potential pozzolanic reactivity. Fig. 2 presents the SEM image of the binder, both OPC and CP are irregular particles. The particle size distribution of the binder is presented in Fig. 3, and the median particle size of OPC and CP are 17.9 and 9.0 μm, respectively. ISO standard sand is used as the fine aggregate, and the water-reducing capacity of polycarboxylate-based superplasticizer (SP) is 25%.

Table 1. Main chemical compositions of the materials (%).

Materials	CaO	SiO_2	Al_2O_3	Fe_2O_3	SO_3	MgO	K_2O	LOI*
OPC	48.16	26.41	6.24	5.02	4.53	2.27	6.24	4.43
CP	52.70	1.70	0.35	0.36	0.61	0.23	0.10	42.38

*LOI: loss on ignition.

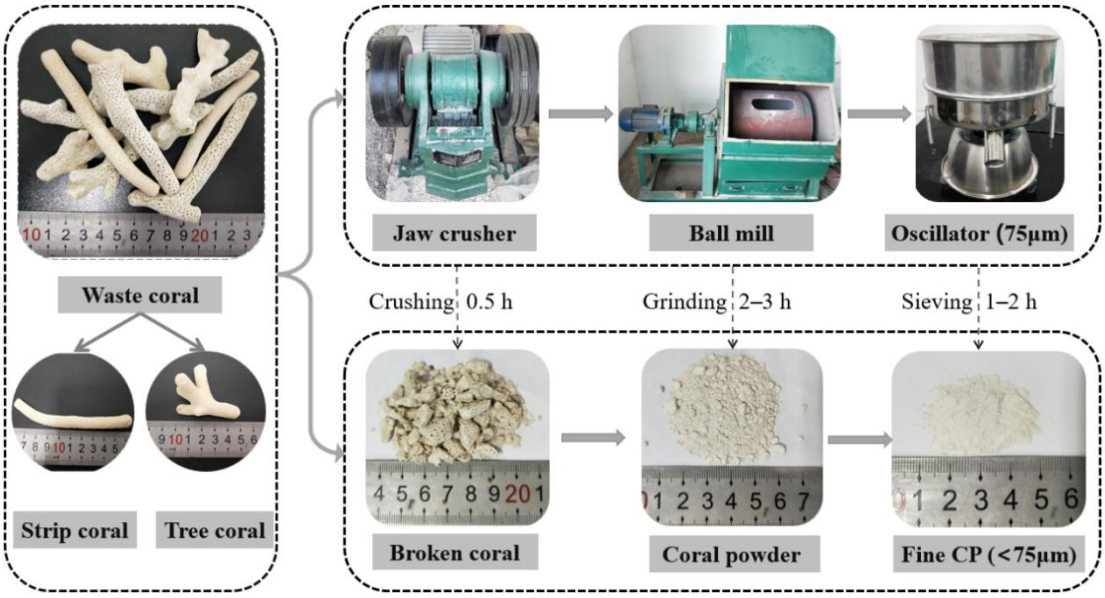

Fig. 1. The preparation process of CP.

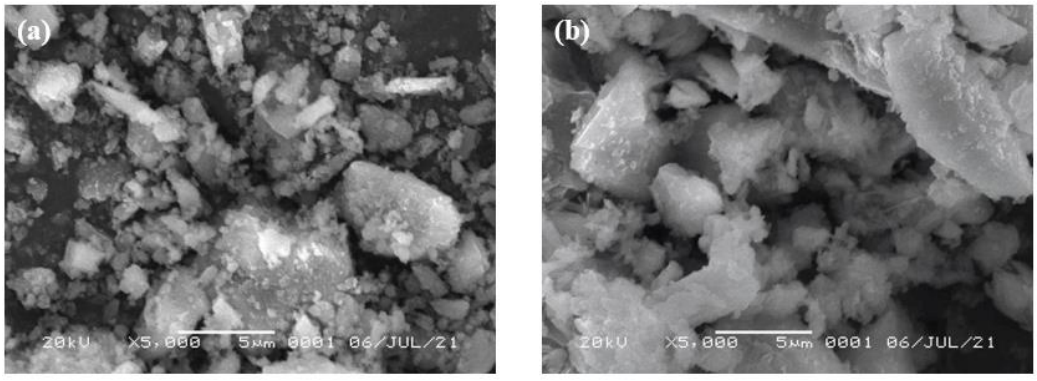

Fig. 2. SEM images of CP (a) and OPC (b).

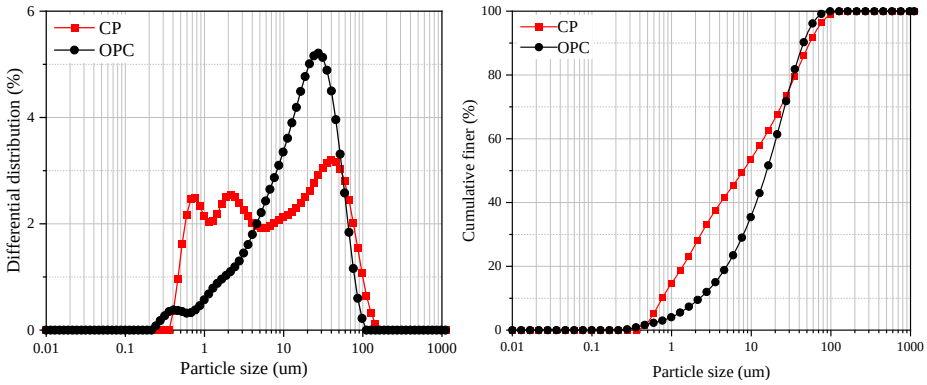

(a) Particle size distributions (b) Grading curves

Fig. 3. Particle size distribution of binder.

2.2. Sample preparation

The mix proportioning design of eco-friendly mortar mixed with high-volume CP is presented in Table 2. To improve the utilization of waste corals during island development, CP is used to replace OPC with the same weight. For all mixtures, the water-to-binder ratio is set at 0.3. To keep the fluidity of the mixture around 150 mm, the amount of SP is 0.9–1.8% of the binder. After 1 d of air curing, the samples are demolded and further cured in a standard curing room with a relative humidity of 98% and a temperature of 20 ± 2 ℃.

Table 2. Mix proportions of HVCM (kg/m^3).

MIX ID	OPC	CP	Sand	Water	SP
M0	450	0	1350	135	8
M20	360	90	1350	135	7
M40	270	180	1350	135	5
M60	180	270	1350	135	4

2.3. Methods

2.3.1. Mechanical properties

According to the standard (GB/T 17671-1999), the compressive strength of the samples (40×40×160 mm) was tested at 7, 28, 60 and 90 d with the loading rate of 2400 N/s. For each strength test, the strength values of the three HVCM samples were averaged.

2.3.2. Autogenous deformation

The corrugated plastic tubes (Φ 29 mm) with a length of 450 mm were used to test the early-ages autogenous deformation of the HVCM mixture according to ASTM C1698-2009. The corrugated plastic tubes were placed on a stand and one end was fixed while the other end was connected to a dial indicator. Dial indicator data were recorded up to 168 h.

2.3.3. Microstructure examination

Scanning electron microscopy (SEM), thermogravimetry (TG) and Brunauer-Emmet-Teller (BET) were used to characterize the microstructure of HVCM samples. The 90-d small piece

132 samples were soaked in isopropanol to stop hydration and then vacuum dried. SEM was used to test
133 the microstructure of the matrix and the interfacial transition zone (ITZ) of sample (3–5 mm) after
134 the surface was sprayed with gold. Dried samples were ground into powder for TG testing with a
135 heating rate of 10 ℃/min until the temperature reached 1000 ℃. Furthermore, the micropores and
136 mesopores of the HVCM samples was analyzed by BET under N_2 environment.
137 2.3.4. Nanoindentation
138 The Hysitron Ti Premier nanoindentation tester was adopted to characterize the
139 nanomechanical properties of the matrix and ITZ of HVCM sample. At 90 d, the samples were cut
140 into cubes with size of 1.5 cm and then impregnated in epoxy resin. The samples were further
141 polished using different fineness polishing compounds, then ultrasonically cleaned and dried.
142 Meanwhile, the roughness of the sample should meet the requirements of R≤100 nm.
143 Based on previous studies, the loading regime and grid were determined [20]. A 10×10 grid
144 was used for the matrix, and the spacing was 5 μm. For ITZ, a 25×4 grid was adopted, which
145 contained a total of 100 test points. For each sample, three test areas were selected and the average
146 value was taken as the test result. For the loading regime, the load was increased from 0 to 4000 μN
147 with a rate of 800 μN/s and held for 2 s, then decreased to 0 with a rate of 800 μN/s.
148 2.3.5. Environmental benefits
149 With the proposal of carbon neutrality strategy, reducing the carbon emission and the utilization
150 of non-renewable energy of concrete materials has become a top priority. Table 3 presents the NREC
151 and CO_2 emission of the raw materials of HVCM mixture, and the total carbon emissions and NREC
152 of the mixture were calculated according to previous studies [21].
153 Table 3. The NREC and CO_2 emission of raw material.

Raw materials	CO_2 emission (kg/kg)	NREC (MJ/kg)	Ref.
Cement	0.85	5.75	[24]
CP	0.01109	0.236	[24]
Sand	0.01	0.0224	[25]
SP	0.3776	11.18	[24]

154
155 **3. Results**
156 3.1. Compressive strength
157 Fig. 4 shows the effect of CP content on the mechanical properties of HVCM samples. As the
158 CP substitution level increases, the strength of the HVCM samples decreases. The 90-d compressive
159 strength of plain mortar (M0) is 54.30 MPa, while those of the HVCM with 20%, 40%, and 60%

CP are 43.56, 23.64, and 20.26 MPa, respectively corresponding to approximately 19.78%, 56.46%, and 62.69% decrease compared to that of the reference specimen. As the CP content increases, the cement content in the HVCM decreases, thereby reducing the content of hydration products per unit volume. Therefore, the dilution effect of CP will inevitably reduce the mechanical properties of cement-based materials, especially for high-volume dosages. It is worth noting that the strength difference between M0 and M20 is not large at 7 d, and the strength gap becomes larger as the curing age increases. At 7 d, the compressive strength of M20 is reduced by 16.5% relative to the reference group, while the gap at 90 d has increased to 19.8%. Yu et al. [7] also found that CP has a positive effect on the strengths of cement samples in the early-ages, and CP provides nucleation sites for cement hydration, thereby improving the early-ages hydration degree of cement. Meanwhile, the filling effect of CP cannot be ignored, and the fine CP particles can refine the pore structure of HVCM. In addition, for cement-based materials incorporating high-volume $CaCO_3$-based SCM, $CaCO_3$ reacts with C_3A to form hydrated calcium carbonate aluminate, thereby inhibiting the conversion of AFt to AFm. In general, AFt has a higher volume than AFm, which is beneficial for filling the pore of the sample [22,26–29].

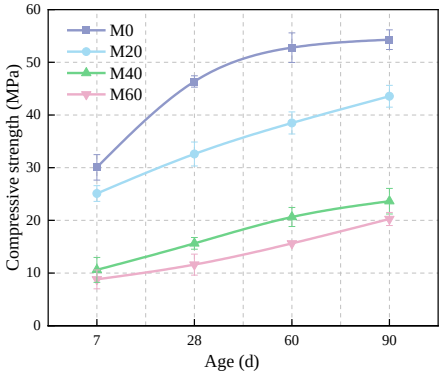

Fig. 4. Mechanical strength of HVCM sample from 7 to 90 d.

3.2. Autogenous shrinkage

Fig. 5 presents the effect of CP content on the autogenous shrinkage of the mixture. As the CP substitution level increases, the autogenous shrinkage value of the mixture decreases significantly. The 168-h autogenous shrinkage value of plain mortar (M0) is 428.21 με/m, while those of the HVCM with 20%, 40%, and 60% CP are 346.79, 273.93, and 183.93 με/m, respectively corresponding to approximately 19.01%, 36.03%, and 57.05% decrease compared to that of the reference sample. The high-volume of CP has a significant dilution effect for the cement paste, which directly reduces the early-ages shrinkage deformation of the sample due to the reduction of

the cement content. It is worth noting that the autogenous shrinkage of the M20 mixture is significantly higher than that of the reference mixture before 35 h, which is related to the fact that CP provides nucleation sites for cement hydration.

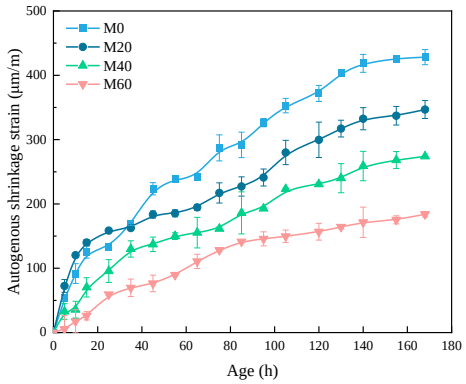

Fig. 5. Autogenous shrinkage of HVCM mixture.

3.3. SEM

Fig. 6 presents the SEM images of 90-d matrix of HVCM sample. For the reference group (M0), its microstructure is relatively dense and mainly composed of C-S-H gel, CH and AFt, etc. As the substitution level of CP increases, the microstructural compactness of HVCM decreases and the pore volume increases. When the substitution level of CP is 40%, the microstructure of the HVCM sample becomes loose and the number of pores increases. With further increase in the CP substitution level, the pore interconnectivity in the samples increases, which leads to an increase in pore diameter. With the increase of CP substitution level, the content of hydration products in HVCM decreases. The incorporation of CP to the sample reduces the relative content of cement and results in a reduction in the content of long-term hydration products of the HVCM. Meanwhile, AFt is also appear in the samples mixed with high-volume CP, indicating that CP inhibits the conversion of AFt to AFm, which may have a positive effect on the densification of the sample microstructure.

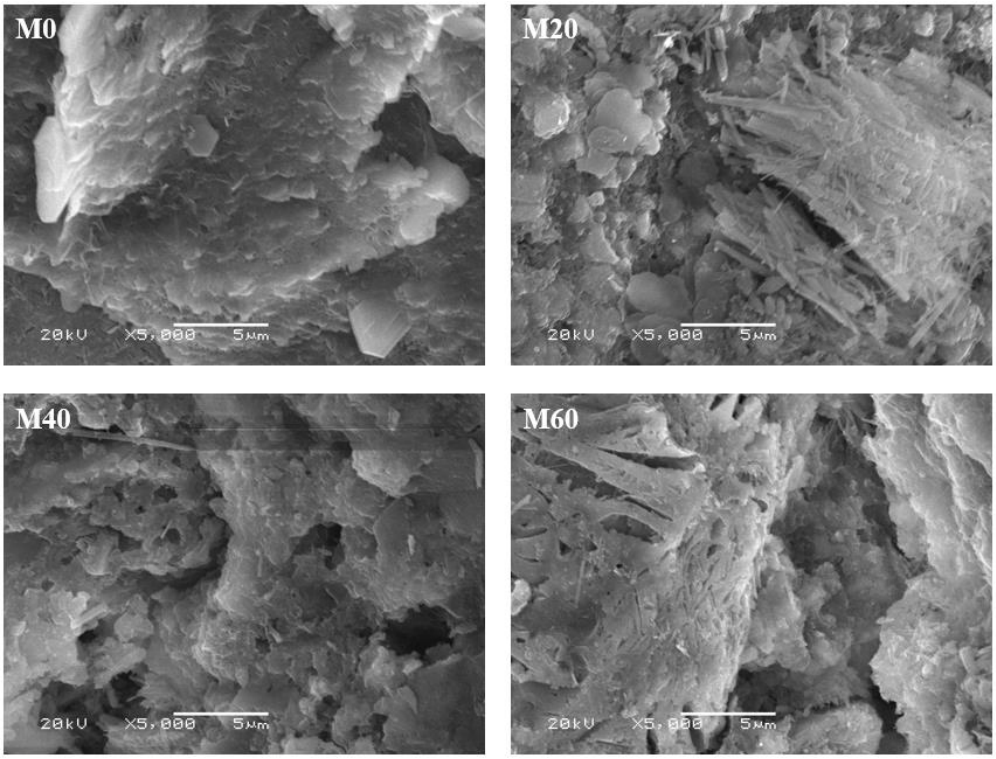

Fig. 6. SEM images of matrix of samples with different CP content at 90 d.

Fig. 7 presents the SEM images of ITZ of HVCM samples at 90 d. Compared to the reference group (M0), the ITZ performance of the M20 sample is slightly degraded. Although the filling effect and pozzolanic reactivity of CP have a positive effect on the compactness of microstructural, the width of ITZ increases due to the decrease of hydration product content. However, it has to be admitted that using SEM to determine the ITZ width of the HVCM samples is still imprecise, so nanoindentation is used to quantitatively characterize the ITZ width of the samples.

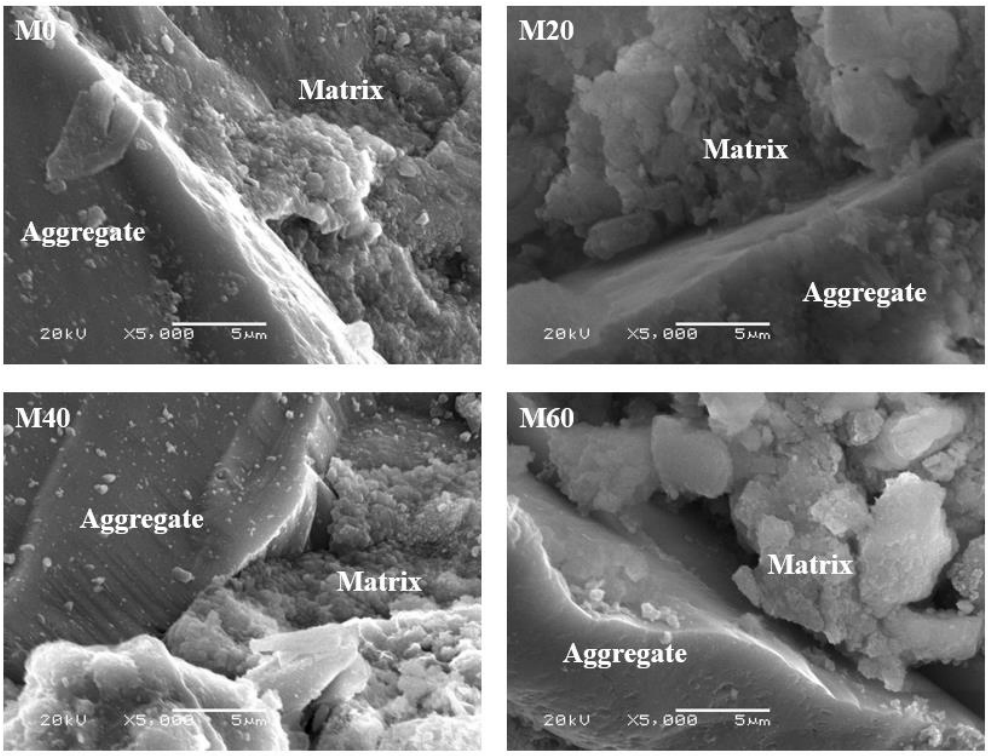

Fig. 7. SEM images of ITZ of samples with different CP content at 90 d.

3.4. Nanomechanical properties

The nanoindentation test is performed on the cement matrix, and its elastic modulus distribution is presented in Fig. 8. According to the difference in elastic modulus of each phase, it can be divided into pore phase (~8 GPa), low density (LD) C-S-H (8–20 GPa), high density (HD) C-S-H (20–35 GPa), CH (35–50 GPa), and unreacted particles (UP) (50~ GPa) [23].

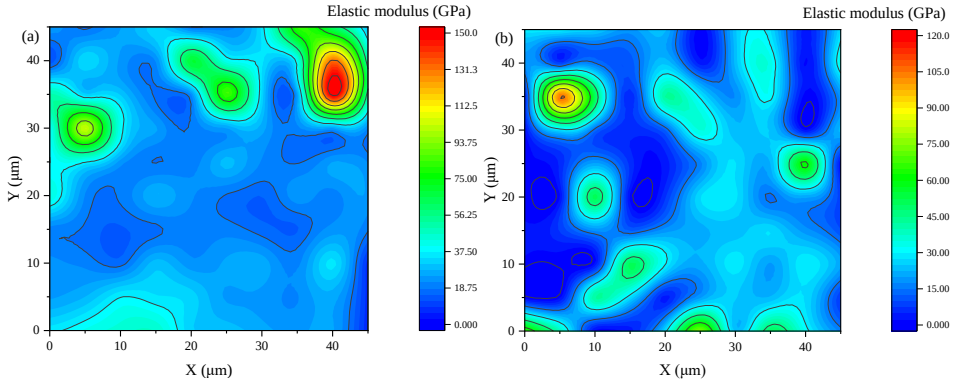

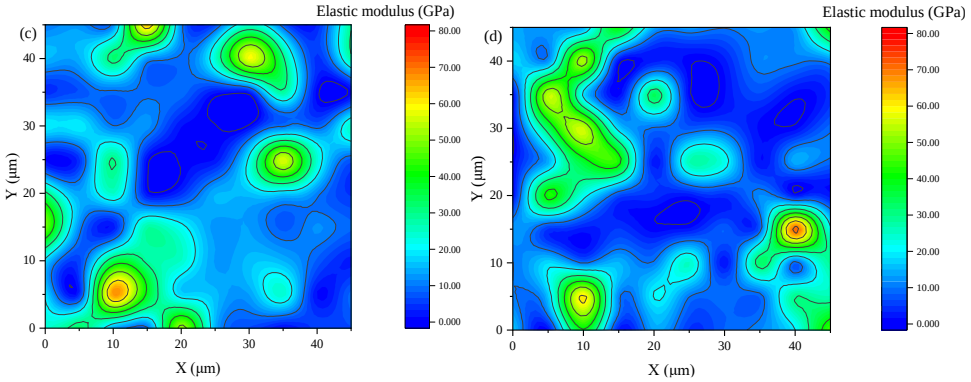

Fig. 8. The distribution of elastic modulus of matrix at 90 d. (a) M0, (b) M20, (c) M40, and (d) M60.

The frequency-stated matrix elastic modulus distribution is fitted by a Gaussian function, and the results are presented in the Fig. 9. As the CP substitution level increases, the color of the cloud map shifts to dark blue, indicating a decrease in the average elastic modulus of the matrix.

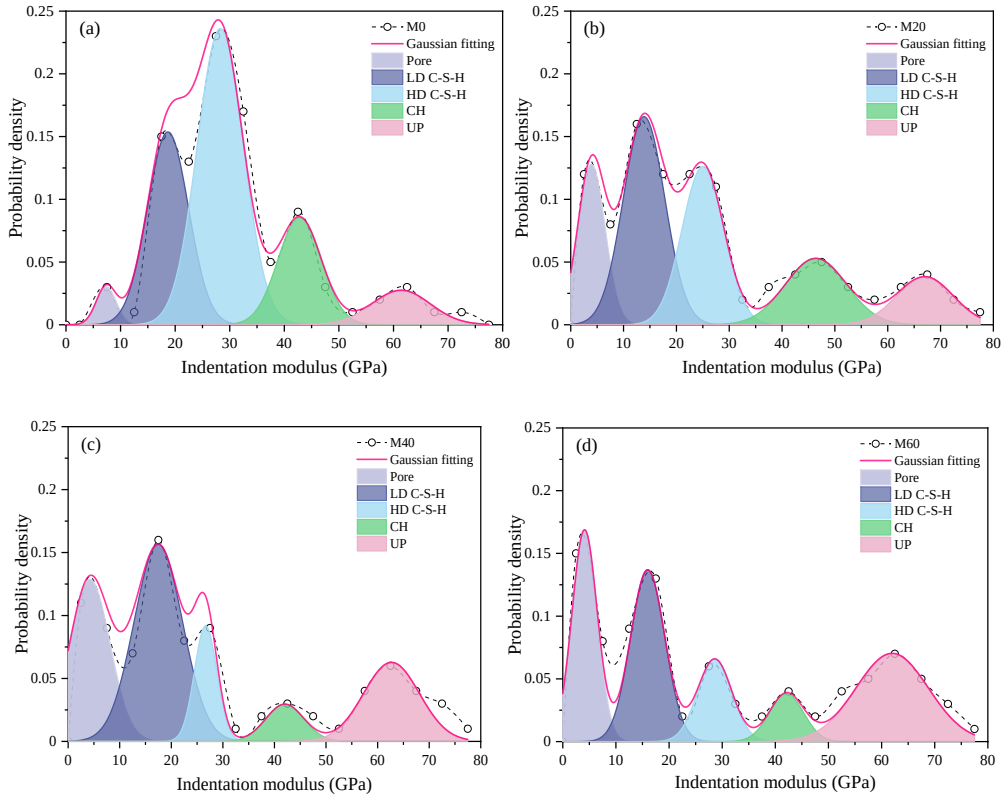

Fig. 9. The frequency distribution of elastic modulus of cement matrix. (a) M0, (b) M20, (c) M40, and (d) M60.

Fig. 10 presents the volume fraction of each phase in the HVCM matrix. With the increase of CP substitution level, the relative content of cement decreases, which leads to a decrease in the content of hydration products (C-S-H and CH) in the matrix. Due to the longer curing age, C-S-H is still the main phase with the highest volume fraction in HVCM. The volume fraction of hydrated phase (C-S-H and CH) of plain mortar (M0) is 88%, while those of the HVCM with 20%, 40%, and

60% CP are 66%, 59%, and 42%, respectively corresponding to approximately 25.00%, 32.95%, and 52.27% decrease compared to that of the reference sample. Meanwhile, with the increase of CP particles, both the volume fraction of unreacted phase and the pore phase increase. It is worth noting that with the increase of CP substitution level, the proportion of LD C-S-H in the C-S-H gel increases, while the proportion of HD C-S-H decreases. This indicates that the use of CP to replace cement reduces the compactness of C-S-H, which may be the main reason for the attenuation of mechanical properties of HVCM sample.

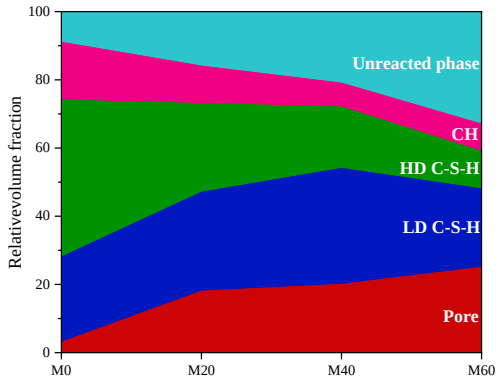

Fig. 10. Effect of CP content on relative content of constituent phases.

The nanoindentation results of ITZ of the HVCM samples are shown in Fig. 11. A weak zone with lower elastic modulus can be found between the aggregate and the cement matrix, which is defined as ITZ. Meanwhile, with the increase of CP substitution level, the width of ITZ of HVCM sample becomes larger. To quantitatively evaluate the ITZ width of the HVCM samples, the elastic moduli of each column were counted, as presented in Fig. 12.

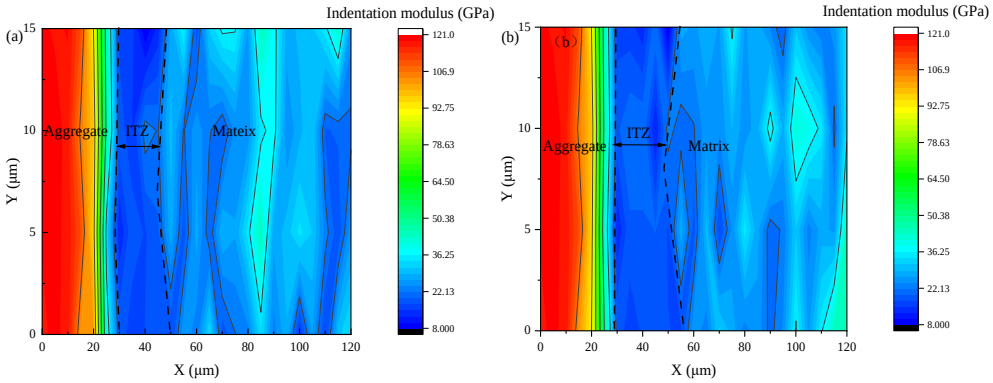

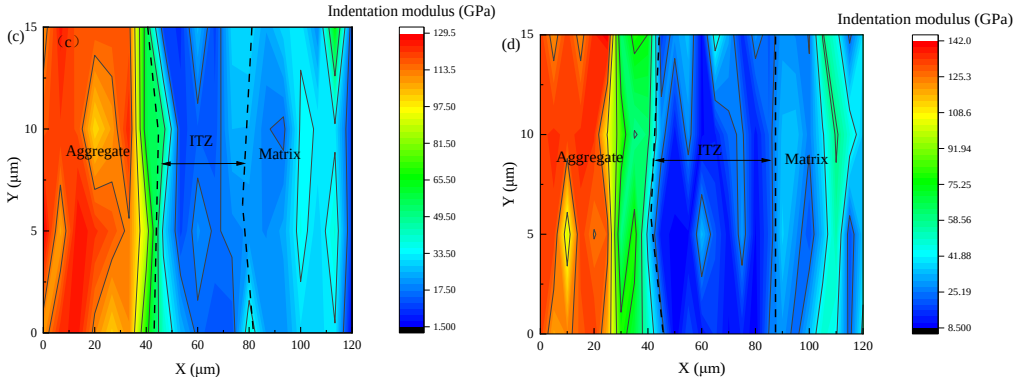

Fig. 11. Contour map of elastic modulus distribution in ITZ of HVCM samples.

From Fig. 12, the ITZ width of the HVCM can be accurately determined. The ITZ width of plain mortar (M0) is 20 μm, while those of the HVCM with 20%, 40%, and 60% CP are 25, 35, and 45 μm, respectively corresponding to approximately 25%, 75%, and 125% increase compared to that of the reference sample. Therefore, as the substitution level of CP increases, the ITZ width of the samples also increases. However, for M20, its ITZ width is only increased by 5 μm compared with the control group, which may also be related to the potential reactivity of CP to inhibit AFm generation.

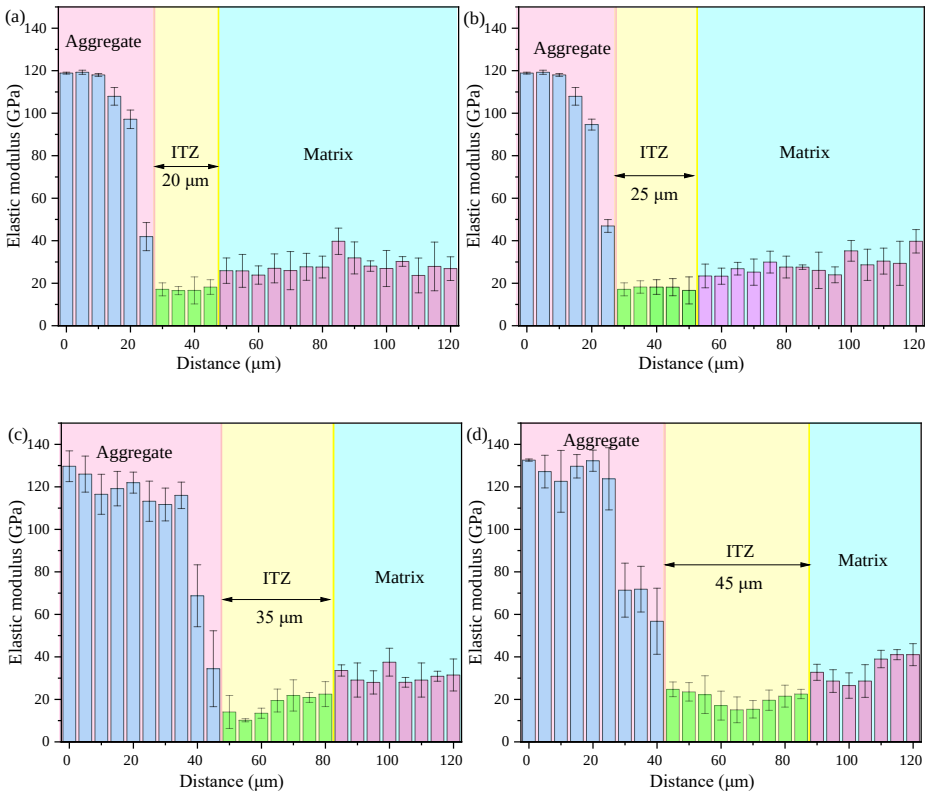

Fig. 12. Effect of CP content on width of ITZ.

4. Discussions

4.1. Influence of high-volume CP on hydration products of cement paste

The effect of CP content on the 90-d hydration product content of HVCM samples is presented in Fig. 13. Decomposition peaks below 100 ℃ are considered to be caused by the decomposition of C-S-H and AFt. The decomposition of monosulfate (AFm) is mainly concentrated at 130–180 ℃. Furthermore, the following two main decomposition peaks are caused by the decomposition of CH (about 450 ℃) and $CaCO_3$ (720 ℃), respectively. As a calcium carbonate mineral, the most intuitive manifestation of incorporating CP to the sample is the increase of $CaCO_3$ content. As the CP substitution level increases, the decomposition peak of $CaCO_3$ also shifts to the right, which indicates that the stability of CP is significantly higher than that of ordinary calcium carbonate. Meanwhile, CP has a significant inhibitory effect on the conversion of AFt to AFm. Even at 90 d, the AFm content in the samples is increased with increasing CP content.

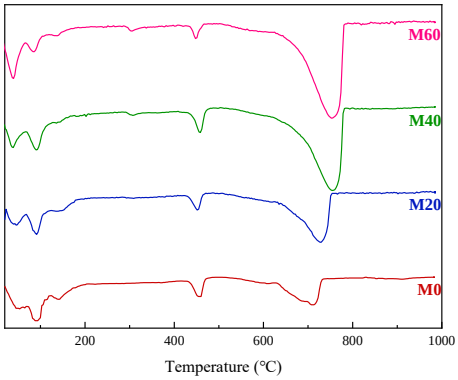

Fig. 13. The DTG curve of cement pastes mixed with CP.

4.2. Influence of high-volume CP on the compactness of C-S-H gel

The microstructure of C-S-H gel is closely related to the strengths and shrinkage deformation behavior of cement samples. BET and nanoindentation techniques are used to characterize the pore structure and compactness of C-S-H gel. As the CP substitution level increases, the porosity of C-S-H also increases due to the decrease in cement content (see Fig. 14). It is worth noting that for M0, M20 and M40 samples, the peak of pore distribution curve of C-S-H shifts towards small size with increasing CP content. This implies that the positive effect of CP in cement hydration plays a key role in its long-term gel pore structure refinement. This is related to CP providing nucleation sites for cement hydration and delaying AFm growth. When the CP substitution level is too high, the pore structure of the C-S-H gel is significantly coarsened.

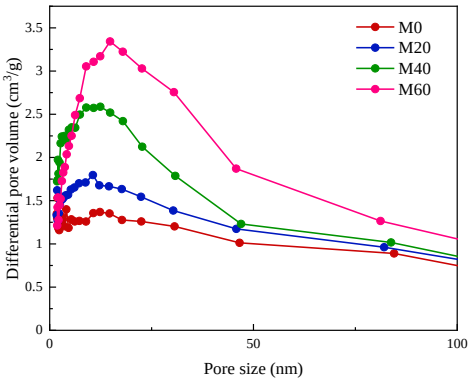

Fig. 14. The pore size distribution of HVCM samples at 90 d.

The average elastic modulus of C-S-H is also closely related to its compactness. Because the substitution level of CP is too high, it does not contribute too much to the densification of C-S-H. With the increase of CP content, the proportion of LD C-S-H increases, and the average elastic modulus of C-S-H decreases (Fig. 15). As the main source of strength, the decrease of elastic modulus of C-S-H gel is also the main reason for the decrease of mechanical properties of the samples.

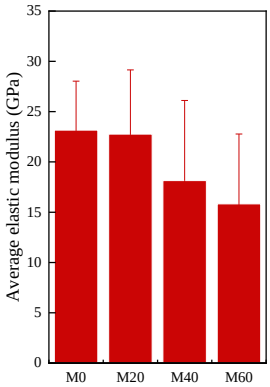

Fig. 15. The average elastic modulus of C-S-H gel.

4.3. Influence of high-volume CP on the environmental benefits of cement mixture

Fig. 16 presents the total carbon emissions and NRECs per cubic meter of HVCM mixture. As the CP substitution level increases, the carbon emission of the mixture decreases significantly. The total carbon emissions of plain mortar (M0) is 399.02 kg/kg, while those of the HVCM with 20%, 40%, and 60% CP are 289.14, 246.88, and 171.00 kg/kg, respectively corresponding to approximately 27.54%, 38.13%, and 57.14% decrease compared to that of the reference specimen. Meanwhile, the effect of CP content on the NREC of HVCM is also similar to that of carbon emission. The NREC of the M60 mixture is only 43.35% of the reference group (M0). Therefore, incorporating a high-volume of CP to cement-based materials can significantly reduce its carbon

emissions and NREC, and HVCM has good environmental benefits.

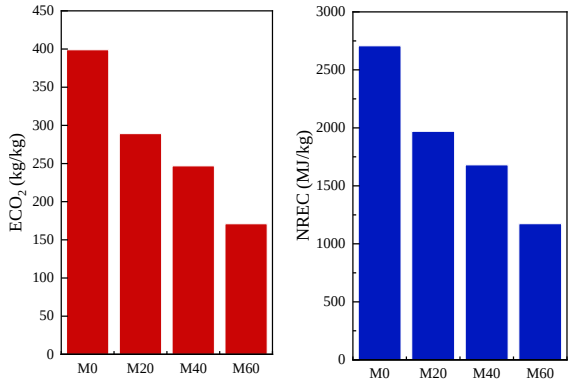

Fig. 16. The effect of CP on the environmental benefits of UHPC mixture.

5. Conclusions

A novel high-volume waste coral powder (CP) mortar (HVCM) was prepared in this study, and its multiscale characteristics were investigated. The obtained results are briefly summarized below.

(1) Although the compressive strength of the mortar is greatly reduced by incorporating high-volume of CP to the mixture, the early-age (7-d) strength and long-term (90-d) strength of HVCM can still reach 83.50% and 80.22% of the plain mortar.

(2) The autogenous shrinkage of HVCM samples is significantly lower than that of ordinary mortar, which is beneficial to reduce the cracking risk of cement-based materials due to autogenous shrinkage. When the substitution level of CP is 60%, the 168-h autogenous shrinkage value of HVCM is decreased by 57.05% relative to the reference sample.

(3) From the nanoscale, with increasing CP substitution levels, the unreacted and pore phases increase, while the relative content of hydration product phases decreases, especially for HD C-S-H. Meanwhile, the increase of ITZ width is also the main reason for the performance degradation of sample with high-volume CP.

(4) Replacing part of the cement with CP inhibits the conversion of AFt to AFm and brings a large amount of calcium carbonate into the system. With the increase of CP content, the pores of the C-S-H gel are increased but the pore size shifted slightly to the smaller size. Meanwhile, CP also reduces the average elastic modulus of C-S-H gel.

(5) Incorporating high-volume CP into cement-based materials is an effective way to reduce carbon emissions and non-renewable energy consumption of the mixture. When the substitution level of CP is 60%, the carbon emissions and energy consumption per cubic meter of the mixture are

only 42.85% and 43.35% of those of plain mortar.

Declaration of Competing Interest

No

Acknowledgements

No

References

[1] Wang, A., Lyu, B., Zhang, Z., Liu, K., Xu, H., Sun, D. (2018a). The development of coral concretes and their upgrading technologies: A critical review. Constr. Build. Mater., 187, 1004-1019.

[2] Wang, A., Zhang, Z., Liu, K., Xu, H., Shi, L., Sun, D. (2019b). Coral aggregate concrete: Numerical description of physical, chemical and morphological properties of coral aggregate. Cement and Concrete Composites, 100, 25-34.

[3] Da, B., Chen, Y., Yu, H., Ma, H., Chen, D., Wu, Z., Li, Y. (2022). Preparation technology, mechanical properties and durability of coral aggregate seawater concrete in the island-reef environment. J. Clean. Prod., 339, 130572.

[4] Fu, Q., Bu, M., Su, L., Guo, B., Chen, L., Song, H., Niu, D. (2021a). Dynamic triaxial compressive response and failure mechanism of basalt fibre-reinforced coral concrete. International Journal of Impact Engineering, 156, 103930.

[5] Ahmad, M. R., Chen, B., Haque, M. A., Oderji, S. Y. (2020). Multiproperty characterization of cleaner and energy-efficient vegetal concrete based on one-part geopolymer binder. J. Clean. Prod., 253, 119916.

[6] Wu, H., Xu, J., Yang, D., Ma, Z. (2021). Utilizing thermal activation treatment to improve the properties of waste cementitious powder and its newmade cementitious materials. J. Clean. Prod., 322, 129074.

[7] Shi, H., Yu, Z., Ma, J., Ni, C., Shen, X. (2019). Properties of Portland cement paste blended with coral sand powder. Constr. Build. Mater., 203, 662-669.

[8] Wang, X., Yu, R., Shui, Z., Song, Q., Zhang, Z. (2017). Mix design and characteristics evaluation of an eco-friendly Ultra-High Performance Concrete incorporating recycled coral based materials. J. Clean. Prod., 165, 70-80.

[9] Nie, Y., Shi, J., He, Z., Zhang, B., Peng, Y., Lu, J. (2022). Evaluation of high-volume fly ash (HVFA) concrete modified by metakaolin: Technical, economic and environmental analysis. Powder Technology, 117121.

[10] Zhang, Z., Wang, Q., Chen, H. (2016). Properties of high-volume limestone powder concrete under standard curing and steam-curing conditions. Powder Technology, 301, 16-25.

[11] Han, F., Wang, Q., Mutian, L., Yingjun, M. (2016). Early hydration properties of composite binder containing limestone powder with different finenesses. Journal of thermal analysis and calorimetry, 123(2), 1141-1151.

[12] Tsivilis, S., Batis, G., Chaniotakis, E., Grigoriadis, G., Theodossis, D. (2000). Properties and behavior of limestone cement concrete and mortar. Cem. Concr. Res., 30(10), 1679-1683.

[13] Fu, Q., Xu, W., He, J., Su, L., Song, H., Niu, D. (2021b). Dynamic strength criteria for basalt fibre-reinforced coral aggregate concrete. Composites Communications, 28, 100983.

[14] Chu, Y., Wang, A., Zhu, Y., Wang, H., Liu, K., Ma, R., Sun, D. (2021). Enhancing the performance of basic magnesium sulfate cement-based coral aggregate concrete through gradient composite design technology. Composites Part B: Engineering, 227, 109382.

[15] Zhou, L., Guo, S., Zhang, Z., Shi, C., Jin, Z., Zhu, D. (2021). Mechanical behavior and durability of coral aggregate concrete and bonding performance with fiber-reinforced polymer (FRP) bars: A critical review. J.

Clean. Prod., 289, 125652.
[16] Gencel, O., Benli, A., Bayraktar, O. Y., Kaplan, G., Sutcu, M., Elabade, W. A. T. (2021). Effect of waste marble powder and rice husk ash on the microstructural, physico-mechanical and transport properties of foam concretes exposed to high temperatures and freeze–thaw cycles. Constr. Build. Mater., 291, 123374.
[17] Howdyshell, P. A. (1974). The use of coral as an aggregate for Portland cement concrete structures. Construction Engineering Research Lab (Army) Champaign IL.
[18] Wang, Y., Shui, Z., Yu, R., Huang, Y. (2018b). Chloride ingress and binding of coral waste filler-coral waste sand marine mortar incorporating metakaolin. Constr. Build. Mater., 190, 1069-1080.
[19] Wang, J., Liu, E., Li, L. 2019c. Characterization on the recycling of waste seashells with Portland cement towards sustainable cementitious materials. J. Clean. Prod., 220, 235-252.
[20] He, Z. H., Han, X. D., Zhang, M. Y., Yuan, Q., Shi, J. Y., Zhan, P. M. (2022). A novel development of green UHPC containing waste concrete powder derived from construction and demolition waste. Powder Technology, 398, 117075.
[21] Shi, J., Tan, J., Liu, B., Chen, J., Dai, J., He, Z. (2021). Experimental study on full-volume slag alkali-activated mortars: Air-cooled blast furnace slag versus machine-made sand as fine aggregates. Journal of Hazardous Materials, 403, 123983.
[22] Lothenbach B., K. Scrivener, R.D. Hooton, Supplementary cementitious materials, Cem. Concr. Res., 41 (12) (2011), pp. 1244-1256.
[23] He, Z. H., Yang, Y., Yuan, Q., Shi, J. Y., Liu, B. J., Liang, C. F., Du, S. G. (2021). Recycling hazardous water treatment sludge in cement-based construction materials: Mechanical properties, drying shrinkage, and nano-scale characteristics. J. Clean. Prod., 290, 125832.
[24] Wang, Y., Shui, Z., Gao, X., Huang, Y., Yu, R., Li, X., Yang, R. 2019a, Utilizing coral waste and metakaolin to produce eco-friendly marine mortar: Hydration, mechanical properties and durability. J. Clean. Prod., 219, 763-774.
[25] Müller, H. S., Haist, M., Vogel, M. (2014). Assessment of the sustainability potential of concrete and concrete structures considering their environmental impact, performance and lifetime. Constr. Build. Mater., 67, 321-337.
[26] Fu, Q., Niu, D., Zhang, J., Huang, D., Hong, M. (2018). Impact response of concrete reinforced with hybrid basalt-polypropylene fibers. Powder Technology, 326, 411-424.
[27] Wang L, Aslani F. Self-sensing performance of cementitious composites with functional fillers at macro, micro and nano scales. Construction and Building Materials, 2022, 314: 125679.
[28] Zhang B, Zhu H, Li F, et al. Compressive stress-strain behavior of seawater coral aggregate concrete incorporating eco-efficient alkali-activated slag materials. Construction and Building Materials, 2021, 299: 123886.
[29] Xu W, Han Z, Tao L, et al. Random non-convex particle model for the fraction of interfacial transition zones (ITZs) in fully-graded concrete. Powder Technology, 2018, 323: 301-309.